Journal of Thermal Engineering
Web page info: https://jten.yildiz.edu.tr
DOI: 10.18186/thermal.1067043

Research Article

Thermal analysis on the impact of spray charactristics on evaporative cooling process

Behzad Siavash AMOLI[1], Seyed Soheil Mousavi AJAROSTAGHI[1], Kurosh SEDIGHI[1]*, Mojtaba Aghajani DELAVAR[1]

[1]Department of Mechanical Engineering, Babol Noshirvani University of Technology, P.O. Box 484, Babol, Iran.

ARTICLE INFO

Article history
Received: 01 April 2021
Accepted: 05 July 2021

Keywords:
Evaporative Cooling Process, Spray, Nozzle, Two-Phase Flow, Droplet, Eulerian-Lagrangian Approach

ABSTRACT

In hot and dry climates, evaporative cooling of the air by water spray can be applied in several requirements, such as evaporative condensers which the airflow is precooled by the water spray before it reaches the condenser. The interaction between water droplets and the air is a complicated two-phase flow that is affected by the several parameters. Here, an Eulerian-Lagrangian 3D model was developed to investigate the influence of important parameters on spray cooling performance in a rectangular duct. The evaluated parameters include the number of nozzles, inlet air flow rate, and spray water flow rate. The results represented that growth in the number of nozzles causes a reduction in the spray cooling efficiency. This is due to decrease of droplets retention time within the duct by increasing the number of nozzles at a constant total spray flow rate in the cases. The maximum and minimum spray cooling efficiency belong to the cases with one nozzle at water flow rate of 20 l/h and four nozzle at water flow rate of 5 l/h, respectively. The difference between spray cooling efficiency at 3 and 4 number of nozzles is less than 1.8%. Moreover, increasing the air flow rate from 0.5 l/h to 2 l/h (by 300%) makes a decrease in the spray cooling efficiency up to 58.6%.

Cite this article as: Behzad S A, Seyed S M A, Kurosh S, Mojtaba A D. Thermal analysis on the impact of spray charactristics on evaporative cooling process. J Ther Eng 2022;8(1):90−102.

INTRODUCTION

Spraying water to cool an air flow is a common phenomenon which has different types of applications in industries such as spray drying, natural draft cooling tower, gas turbine fogging, air conditioning and firefighting [1]. In a spray cooling process, the water small droplets are injected into an air flow, this increases the contact surface area between water droplets and air, so higher rate of sensible heat transfer and evaporation will be occurred [2]. Therefore, by spraying water droplets into the air, temperature declines and humidity increases, so this concept is appropriate for hot and dry climates.

The interaction between a continuous air flow and dispersed water droplets in a spray cooling process, is a complicated two phase flow which is affected by a lot of

***Corresponding author.**
*E-mail address: ksedighi@nit.ac.ir

This paper was recommended for publication in revised form by Regional Editor Ahmet Selim Dalkilic

Published by Yıldız Technical University Press, İstanbul, Turkey

parameters taken part in mass, momentum and energy exchange between two phases. Detailed data on the influence of spray cooling characterization is essential for designing an effective evaporative cooling system for several engineering applications. Dry bulb temperature, ambient absolute humidity, air flow velocity, temperature and velocity of droplets are the main operational parameters which influence on the spray cooling performance. A number of papers with experimental [3-6] or numerical [7-10] analysis, focused on the investigation of operational parameters impress on the spray cooling performance.

Because of the complexity of two phase flow in evaporative cooling and participation of a lot of attendant parameters in it, numerical studies are more prevalent than the experimental studies [11]. These numerical investigations were carried out for inlet air flow of cooling towers, hot plates, air-cooled condensers, heat exchangers and other thermal components [12–15].

According to different conditions of each application, it is necessary to study spray cooling process, for any usage separately with its specification. In order to investigate evaporative cooling in a specified condition, a number of studies use a wind tunnel and a spray system with different characteristics. Alhkhedir et al. [16] performed a parametric study on a spray cooling system for optimization of nozzle design applied in natural draft dry cooling towers. The results indicated that initial droplet velocity is an important parameter which influences on spray cooling performance. As droplets velocity increases, the spray cooling efficiency improves. Complete evaporation was achieved for an optimum initial droplet velocity, which for higher measurement of this parameter no enhancement was observed in spray cooling. In another study, a numerical model was developed by Montazeri et al. [17] to study the effect of inlet air dry bulb temperature and ambient relative humidity on the spray cooling efficiency. They put a spray nozzle within a wind tunnel in co-current condition with the air flow. The results showed that for a certain value of inlet water droplet temperature, increasing 8°C in inlet air dry bulb temperature, enhances the sensible cooling capacity of the system, more than 40%. Moreover, a lower amount of humidity in the inlet air flow, augments the evaporation rate and improves spray cooling. CFD analysis of pre-cooling by a water spray system in horizontal nozzle arrangements was carried out by Xia et al. [18]. Main conclusion was that, the maximum fully evaporated water flow, witnesses a decrease with increasing the air velocity and the growth of turbulence intensity could improve evaporative cooling capacity by enlarging spray coverage area.

The influence of inlet water temperature on the cooling efficiency of a water mist fire suppression system has been analyzed by Omidvar et al. [19]. The spray system had one nozzle in co-current condition with the air stream. Results represented that when the initial temperature of the water spray before injection increases, the initial size distribution of the spray droplets decreases and the speed of droplets evaporation augments therefore cooling power of the preheated water mist system improves.

Air-cooled condenser is another thermal component which its performance can be enhanced by spray pre-cooling of its air flow in hot and dry weather. Heidarinejad et al. [20] investigated the effect of air spray cooling to enhance the performance of an air-cooled chiller with integrating a water mist system to its condenser. They applied one nozzle in the water mist system with different nozzle orientation angles from 0 to 90°. The main result of this study is that for the higher ambient temperature, COP enhancement is better and at orientation angle of 90° the best cooling was observed. Xiao et al. [21] performed a numerical study on performance improvement of an air-cooled condenser by water spray cooling. The results showed that for high ambient dry bulb temperatures and low relative humidity, the spray cooling capacity is more. A new type of evaporative condenser with water spray cooling is used in a data center air conditioning system by Han et al. [22]. Results represented that, the evaporative condenser can decrease the energy consumption of the system, and increase the COP of air conditioner

The literature review showed that in most numerical studies, the condition of air stream relative to spray direction was co-current, while according to the represented results by Heidarinejad et al. [20], the orientation angle of 90° for spray nozzle is more efficient than the other configuration. Therefore, the condition of present study is assumed cross flow which is more effective and poorly highlighted in the literature. Moreover, to the best of author's knowledge, it has not been found any study which investigate the effect of number of nozzles on pre-cooling of an air flow by a spray system, therefore in the present work the influence of number of nozzles is comprehensively analyzed on spray cooling efficiency and evaporation rate. Also the spray mass flow rate and inlet air flow rate, as two important operational parameters are variable in this study which their effect in cross flow configuration and more than one nozzle condition have not been investigated yet. In order to perform the numerical analysis, a number of 32 cases were simulated with different number of nozzles, air and water mass flow rate. Two-phase Eulerian-Lagrangian model is utilized to simulate the heat transfer and fluid flow of water spray process inside the air flow. The applied two-phase model has been validated by the results of a previous reliable work.

NUMERICAL MODEL

There are two phases in the domain of the model; continuous phase and discrete phase which are the air flow and spray droplets, respectively.

Continuous Phase

According to the Eulerian-Lagrangian model, the simulation of air flow is described in Eulerian framework. The continuity equation with source term and the Reynolds-Averaged Navier-Stokes (RANS) momentum and energy equations with the combination of standard k-ε model are used to simulate the air flow which is in contact with water droplets. These equations are as follow [23]:

$$\frac{\partial\left(\rho v_i\right)}{\partial x_j}=S_m \tag{1}$$

$$\frac{\partial\left(\rho v_i v_j\right)}{\partial x_j}=\rho\vec{g}-\frac{\partial P}{\partial x_j}+\frac{\partial}{\partial x_j}\left[\mu\left(\frac{\partial v_i}{\partial x_j}+\frac{\partial v_j}{\partial x_i}\right)-\frac{2}{3}\mu\delta_{ij}\left(\frac{\partial v_j}{\partial x_i}\right)\right]+S_{mo} \tag{2}$$

$$\rho v_i\frac{\partial E}{\partial x_j}=-P\frac{\partial v_i}{\partial x_j}+\frac{\partial}{\partial x_j}\left(\sum_i^n h_i J_i\right)+\frac{\partial}{\partial x_j}\left(K_a\frac{\partial T}{\partial x_j}\right)+\Phi+S_e \tag{3}$$

$$\rho v_i\left(\frac{\partial\left(Y_j\right)}{\partial x_j}\right)=\frac{\partial J_{i',i}}{\partial x_j}+S_m \tag{4}$$

The airflow is treated as steady, turbulent and incompressible. The source terms S_{mo}, S_e, S_m which indicate the mass, momentum, and energy effects of dispersed droplets on the continuous air flow, are evaluated in Lagrangian framework. Actually, the process of one iteration of simulation is that the continuous phase equations are solved without discrete phase source terms then discrete phase relations are computed and the source terms are evaluated then continuous phase equations with source terms will be solved, if the convergence conditions is satisfied the calculation will be stopped otherwise the iterations continue.

In the finite volume simulation, for each computational cell, the source term is calculated by volume averaging of the impact of droplets within the cell, on the airflow. These source terms are derived as follow:

$$S_m=-\frac{1}{V_{cell}}\sum_n\frac{d\left(m_d\right)}{dt} \tag{5}$$

$$S_{mo}=-\frac{1}{V_{cell}}\sum_n\frac{d\left(m_d V_d\right)}{dt} \tag{6}$$

$$S_e=-\frac{1}{V_{cell}}\sum_n\frac{d\left(m_d E_d\right)}{dt} \tag{7}$$

Discrete Phase Model

In the spray cooling process, the mass, momentum, and energy exchange of the water droplets which is injected to the airflow directly depends on the interaction between the two phases. Momentum exchange causes the droplet motion, mass transfer determines droplet size change and energy exchange influences on the droplets temperature.

DROPLET EQUATIONS OF MOTION

The droplets equation of motion is computed in Lagrangian framework. The trajectory of some droplets which have the same properties, named parcels, is traced in the continuous air flow domain [24]. The particles equations of motion are derived by integration over second law of Newton in three dimensions. When the water droplets inject to an air flow, there are a lot of forces which exerts to them. These forces are such as drag, gravity, buoyancy, thermo-phoretic, Brownian, and Saffman's lift forces [20]. When it is assumed that the droplets have spherical shape, the drag and gravitational forces are more important and the other forces can be neglected [25]. So, the droplets equation of motion in Lagrangian framework is represented as follow:

$$\frac{du_d}{dt}=F_D\left(u_a-u_d\right)+\frac{g_x\left(\rho_d-\rho_a\right)}{\rho_d} \tag{8}$$

$$\frac{dv_d}{dt}=F_D\left(v_a-v_d\right)+\frac{g_y\left(\rho_d-\rho_a\right)}{\rho_d} \tag{9}$$

$$\frac{dw_d}{dt}=F_D\left(w_a-w_d\right)+\frac{g_z\left(\rho_d-\rho_a\right)}{\rho_d} \tag{10}$$

The drag force vector for spherical shape droplets can be derived as Equation (11):

$$\overrightarrow{F_D}=-\frac{\pi}{8}C_D\rho_a D_d^2\left|\overrightarrow{V_a}-\overrightarrow{V_d}\right|\left(\overrightarrow{V_a}-\overrightarrow{V_d}\right) \tag{11}$$

with the assumption of spherical droplets, the drag coefficient, C_D, is only a function of Reynolds number. There are different correlations for the drag force coefficient of spherical droplets in previous studies [26–28]. In this work, a correlation which is developed by Morsi and Alxander [29] is chosen as follow:

$$C_D=\frac{C_1}{Re_d}+\frac{C_2}{Re_d^2}+C_3 \tag{12}$$

where Re_d is the relative Reynolds number between the air flow and the droplets which is given:

Table 1. Morsi and Alexander drag coefficient constant [29]

Re range	C_1	C_2	C_3
$Re_d < 0.1$	24	0	0
$0.1 < Re_d < 1$	22.73	0.09	3.69
$1 < Re_d < 10$	29.17	−3.89	1.22
$10 < Re_d < 100$	46.50	−116.67	0.62
$100 < Re_d < 1000$	98.33	−2778	0.36
$1000 < Re_d < 5000$	148.62	−47500	0.36
$5000 < Re_d < 10000$	−490.546	578800	0.46
$10000 < Re_d < 50000$	−1662.50	5416700	0.52

$$Re_d = \frac{\rho_a D_d \left|\overrightarrow{V_a} - \overrightarrow{V_d}\right|}{\mu_a} \tag{13}$$

The constants C_1, C_2, and C_3 are represented in Table (1) for different ranges of Reynolds number:

DROPLET DIAMETER DISTRIBUTION

The Rosin-Rammler model is applied to depict the size distribution of the droplets in the numerical simulations. This model supposes an exponential relationship between the droplet diameter, D, and the mass fraction of droplets with diameters greater than D, which can be expressed as [17]:

$$Y_D = e^{-\left(\frac{D}{\bar{D}}\right)^n} \tag{14}$$

where Y_D is the mass fraction of droplets with diameters greater than D and $\bar{D}$ is the mean droplets diameter and n is the spread parameter as an index of the distribution width. For the common experimental data, $\bar{D}$ and n are 369 μm and 3.67, respectively. The Rosin-Rammler volume density distribution of the droplets can be derived as follows:

$$f_3(D) = \frac{n}{\bar{D}}\left(\frac{n}{\bar{D}}\right)^{n-1} . e^{-\left(\frac{D}{\bar{D}}\right)^n} \tag{15}$$

The total number of droplet streams in the simulations is assumed to be 100. It means that the particles are released from 100 uniformly distributed points on the nozzle discharge perimeter. The results of sensitivity analysis which is carried out before the main runs, show that approximately 100 streams are needed to obtain CFD result which are independent of the number of droplet streams. In the other words, using a larger number of streams would increase the computational time without any considerable effect on the accuracy of CFD results. Using a lower number of streams, however, would lead to a high discrepancy between the CFD results. In this study, the smallest droplet diameter to be considered in the size distribution of the Rosin-Rammler model is 74 μm, corresponding to the minimum resolution of the droplet measurements. The largest droplet diameter is considered 518 μm, based on the largest droplet diameter in the samples [17].

DROPLET HEAT AND MASS TRANSFER

Whenever a water droplet confronts with an unsaturated airflow, heat and mass transfer happens at its external surface simultaneously. There is latent heat transfer because of droplet evaporation and sensible heat transfer caused by convection and radiation, at the droplets and surrounding air interface. Convection and radiation heat transfer methods are negligible in comparison to the latent heat transfer caused by evaporation [30]. The energy balance over a droplet in contact with an airflow can be expressed as:

$$m_w c_w \frac{dT_d}{dt} = h_c S_d \left(T_a - T_d\right) - \frac{dm_d}{dt} h_{fg} \tag{16}$$

The left hand side of Equation (16) indicates the internal energy variation rate of the droplet and the right hand side includes airflow and the particle convection heat transfer rate and the droplet evaporation rate. The average Nusselt number are obtained as [31]:

$$Nu = \frac{h_c D}{k_a} = 2 + 0.6\, Re_d^{0.5} Pr^{0.33} \tag{17}$$

The term $\frac{dm_d}{dt}$ which represents the mass reduction rate of water droplet caused by evaporation is expressed as Equation (18).

$$\frac{dm_d}{dt} = S_d h_d \left(\rho_{s,int} - \rho_{va}\right) \tag{18}$$

where $\rho_{s,int}$ and ρ_{va} are the saturated vapor – air layer density and vapor density, respectively. The mass transfer coefficient, h_d, can be calculated by Equation (19) [31]:

$$\frac{h_d D}{D_f} = 2 + 0.6\, Re_d^{0.5} S_c^{0.33} \tag{19}$$

Spray cooling efficiency and area averaged air temperature and percentage of water evaporated are the output data of this study. The cooling efficiency of a spray system is determined as the ratio of the real air temperature drop to the maximum probable air temperature drop [32]. It can be obtained from Equation (20):

$$\eta_{sc} = \frac{T_{a,in} - T_{a,out}}{T_{a,in} - T_{wb}} \tag{20}$$

The area averaged temperature can be expressed as:

$$T_{ave} = \frac{\int T dA}{\int dA} \quad (21)$$

According to DPM model of ANSYS Fluent which is applied in this study, the percentage of water evaporated is computed from division of the number of evaporated droplets to the total number of droplets tracked. These information is represented in console dialog box in ANSYS Fluent.

GEOMETRY, PHYSICAL SPECIFICATION AND GRID GENERATION

The computational domain is a channel with dimensions 67.5 × 67.5 × 200 cm^3 which is indicated in Figure 1. The number of the nozzles is variable in the simulation process and the state of four hollow cone nozzles is displayed in Figure 1. The other states are generated by removing the nozzles closer to the outlet of channel. The nozzles are located in the top side of the channel with distances of 0.2, 0.6, 1 and 1.4 m from the inlet. Water droplets are sprayed in cross flow condition. Two boundary conditions including VELOCITY_INLET and PRESSURE_OUTLET are considered for inlet and outlet ports, respectively. The other boundaries are considered as Wall. A structured hexahedral mesh is generated in ICEM CFD. The grid dependency test was carried out on three sizes of mesh and the results are shown in Table 2. Since the difference between the outlet areas averaged temperature of air flow in 1,245,000 elements and 2,050,000 elements is insignificant by 0.01%, and this difference for area averaged water mass fraction at the outlet is zero, the mesh with 1,245,000 elements is chosen for further simulations.

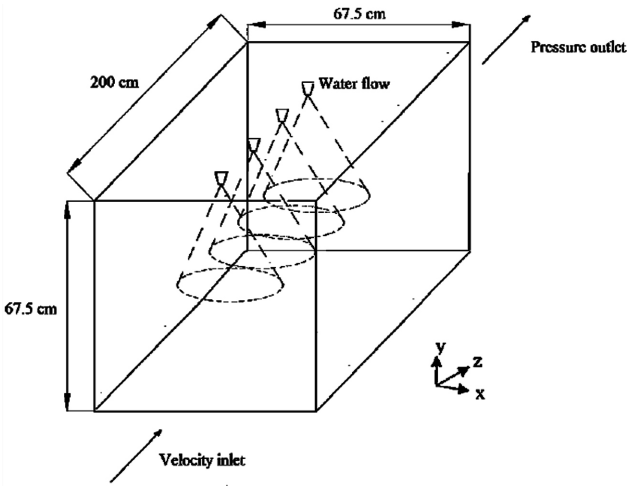

Figure 1. Schematic of the channel geometry and the placement of the nozzles at z=0.2, 0.6, 1, and 1.4 m.

The numerical analysis is performed by a commercial CFD code, ANSYS FLUENT 18.2. The Lagrangian-Eulerian approach with discrete phase model (DPM) is implemented to simulate the sprayed droplets and air flow interaction. In DPM model, the concept of particle stream or parcel is applied for droplet trajectory. Each particle stream is actually a number of droplets which has the same physical properties such as diameter, velocity, and temperature. According to the sensitivity analysis, the number of streams is considered 300 and simulation represented that, for number of streams more than 300, there is no significant difference between the obtained results. The continuous phase 3-D incompressible, steady, and pressure based equations with gravity source term is considered as general specifications of model. Turbulence Reynolds Averaged Navier-Stokes equations with the k-ε model [33–40] is supposed to solve the conversation of mass, momentum, and energy equations of the model. The SIMPLE algorithm is used to solve pressure and velocity coupling equations. The physical parameters of continuous and discrete phases are represented in Table 3.

Table 2. Results of grid dependency study

Grid	Min size (m)	Max face size (m)	Max Tet size (m)	elements number	$T_{a,out}$ (K)	Outlet water mass fraction
1	10^{-4}	10^{-2}	0.02	746,953	306.24	1.35×10^{-3}
2	9×10^{-5}	9×10^{-3}	0.015	1,245,442	306.03	1.36×10^{-3}
3	8×10^{-5}	8×10^{-3}	0.01	2,051,780	306	1.36×10^{-3}

Table 3. Air and spray flows characteristics

Airflow Physical Parameters			Spray System Physical Parameters				
$T_{a,in}$ (K)	$u_{a,in}$(m/sec)	RH_{in}	$m_{w_{tot}}$ (l/h)	v_d	α	D_n	N
308.15	0.5, 1, 1.5, 2	35%	5, 10, 15, 20	10 *m/sec*	30°	0.3 *mm*	1, 2, 3, and 4

The inlet air flow with uniform air velocity, constant relative humidity, and constant dry bulb temperature is determined. The turbulence hydraulic diameter and intensity is considered 0.675 m and 10%, respectively.

BOUNDARY CONDITIONS

Uniform and constant velocity is assumed for airflow boundary condition at the inlet. Atmospheric pressure is set for the outlet. The escape boundary condition is considered for the droplets at the outlet. By using this condition, the upstream effect of the drift eliminator on airflow is ignorable and the particles leave the channel with their current physical properties. No slip condition and reflected boundary condition is assumed for the wall of the channel. When reflected boundary condition is supposed, it means that after droplets impingement to the wall, the normal momentum part will be imposed to zero and the tangential part retains its amount of before collision.

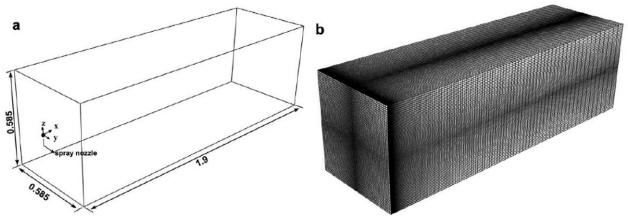

Figure 2. Schematic Geometry (a) and grid generation (b) of the reference case of validation [17].

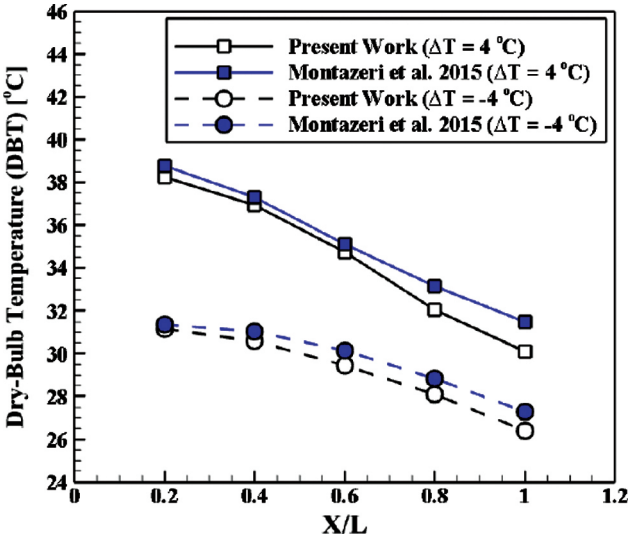

Figure 3. Comparison between present numerical results and Montazeri et al. [17] at V_{air}= 3 m/sec and $U_{droplet}$ = 22 m/sec.

VALIDATION STUDY

Montazeri et al. [17] developed a 3D two-phase model for simulation of air flow in a channel with spray injection at the inlet of the channel in co-current pattern. The dimensions of the channel were 0.585 m × 0.585 m × 1.9 m and its computational domain and grid generation is demonstrated in Figure 2.

In order to validate the utilized model in the present work, a comparison was performed between the results of this model with Montazeri et al. [17] simulation. In the reference case, inlet air velocity, air absolute humidity and water droplet temperature are 3 *m/sec*, 0.0052 $kg_{vapor}/kg_{dry\text{-}air}$, and 308.3 K, respectively. Inlet air dry bulb temperature was assumed as 304.3 K and 312.3 K. Figure 3 represents the area averaged air dry bulb temperature in five cross section of the computational domain in the channel. It shows a very good agreement between the results. The minimum and maximum deviation of the temperatures are 0.6 and 4.7%, respectively.

UNCERTAINTY ANALYSIS

Numerical simulation of Montazeri et al. [17] by itself, was validated with an experimental work carried out by sureshkumar et al. [41]. The uncertainty in measurement of the experimental parameters was as follows. The uncertainty in air velocity measurement was ±0.05*m/s* for air velocity up to 2 *m/s* and ±0.2 *m/s* for air velocity between 2 and 4 *m/s*. The uncertainty of air dry bulb temperature was ±0.3°C in this study. The droplet diameter distribution was determined using an image-analyzing technique. The uncertainty of this technique for the mean droplet size was estimated to be ±22%.

RESULT AND DISCUSSION

In this section, the distribution of dry bulb air temperature, percentage of water droplets evaporation at the outlet, and the spray cooling efficiency have been obtained for different number of nozzles, various inlet air velocities, and different mass flow rates of sprayed water.

IMPACT OF THE NUMBER OF NOZZLES

The number of the nozzles is a key parameter which can affect the spray cooling performance. The impact of number of the nozzles on evaporative cooling process is investigated by testing one to four nozzles in specified locations in the top wall of the duct. The air temperature contours in a longitudinal plane at the middle of the channel (Y=0) for 1 to 4 number of the nozzles on a line with 0.2, 0.6, 1, and 1.4 m distance from the inlet, are illustrated in Figure 4. For each nozzle, the water flow rate and inlet air velocity are kept constant by 5 l/h and 0.5 m/s, respectively. Accordingly, it can be concluded that when the number of the nozzles increases,

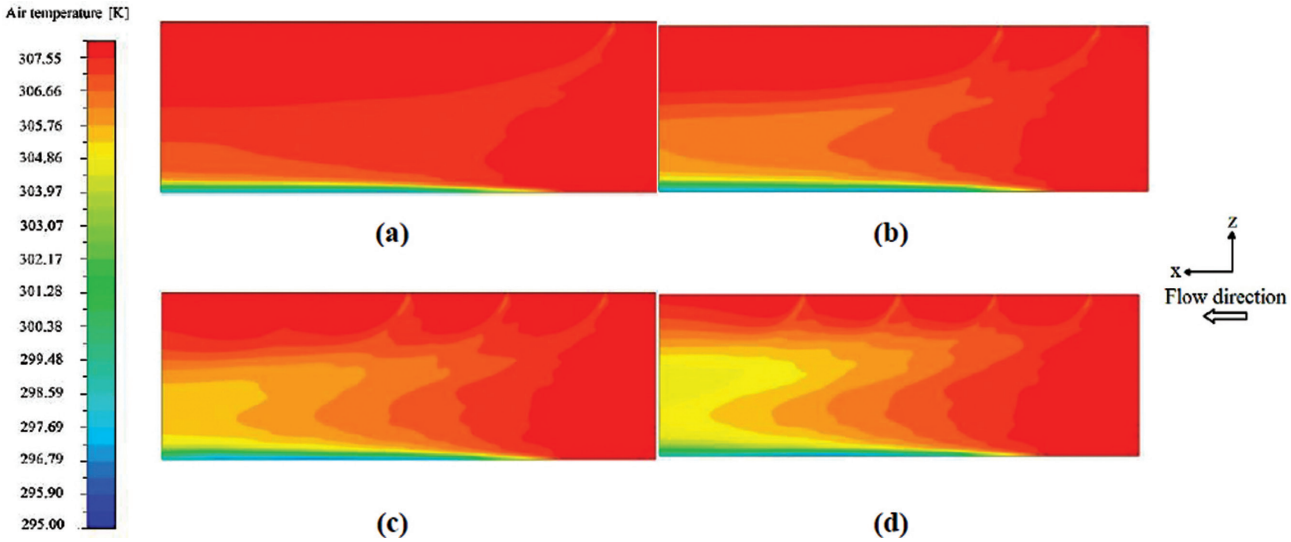

Figure 4. Air temperature profile at the middle longitudinal plane ($u_{a,in}$ = 0.5 *m/sec* and $\dot{m}_w$ = 5 *l/h* for each nozzle) for various number of nozzles including (a) N=1, (b) N=2, (c) N = 3, and (d) N = 4.

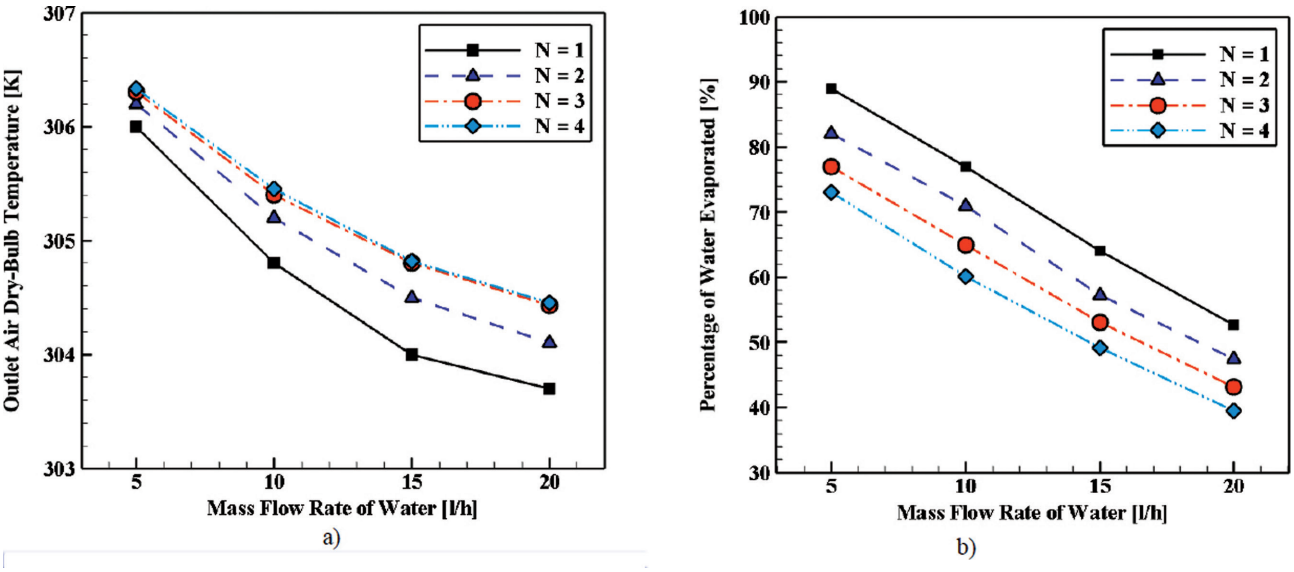

Figure 5. Variation of (a) outlet air dry-bulb temperature and (b) percentage of water evaporated at different water mass flow rates and various numbers of the nozzles.

the amount of sprayed water droplets which is injected into the channel rises, therefore the sensible and latent heat transfer increase because of the water droplets injection, and a greater part of the duct is impressed by spray cooling. It is necessary to mention this point that according to Figure 4, the differences between the cases N=3 and N=4 are not significant which means that growth in the number of spray nozzles more than three does not affect the cooling process expressively.

In the contours of Figure 4, as the spray mass flow rate was assumed 5 l/h for each nozzle, by increasing the number of nozzles, the total mass flow rate grows subsequently, while in order to investigate the effect of number of the nozzles independently, the total mass flow rate for the cases should be constant and it is distributed between the nozzles. In the simulation cases of Figure 5 and Figure 6, for example at total mass flow rate of 10 l/h, when there are two nozzles in the duct, each of them has 5 l/h flow rate and in

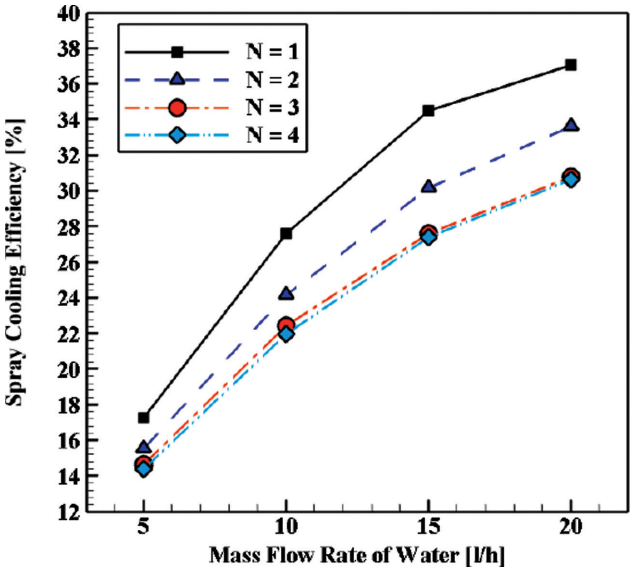

Figure 6. Variation of the spray cooling efficiency at different water mass flow rates and various numbers of the nozzles.

the case of four nozzles, each nozzle injects water spray in amount of 2.5 l/h.

According to the Figure 5(a), at a constant total mass flow rate, when the number of the nozzles increases, the outlet air temperature rises. In other words, when just the number of spray nozzles changes and the other parameters including total spray flow rate, air velocity, droplet size, and inlet air humidity are kept constant, if the number of the nozzles increases on a line in the duct, the mass flow rate of water in each nozzle decreases. So for the nozzles which is closer to the outlet of the duct, the time of interaction between air flow and the water droplets declines which leads to lower heat transfer rate in both sensible and latent types and consequently, the outlet air temperature will be stayed high. Also, according to Figure 5(a), it can be concluded that by growth in the number of the nozzles from 1 to 4 (by 300%), the slope of variation of outlet air temperature reduces, such a way that, the difference between the outlet dry bulb temperature at 3 and 4 number of nozzles is less than 0.05 K. Figure 5(b)shows that the percentage of the water evaporated reduces by increasing the number of the nozzles because when the spray droplets have less residence

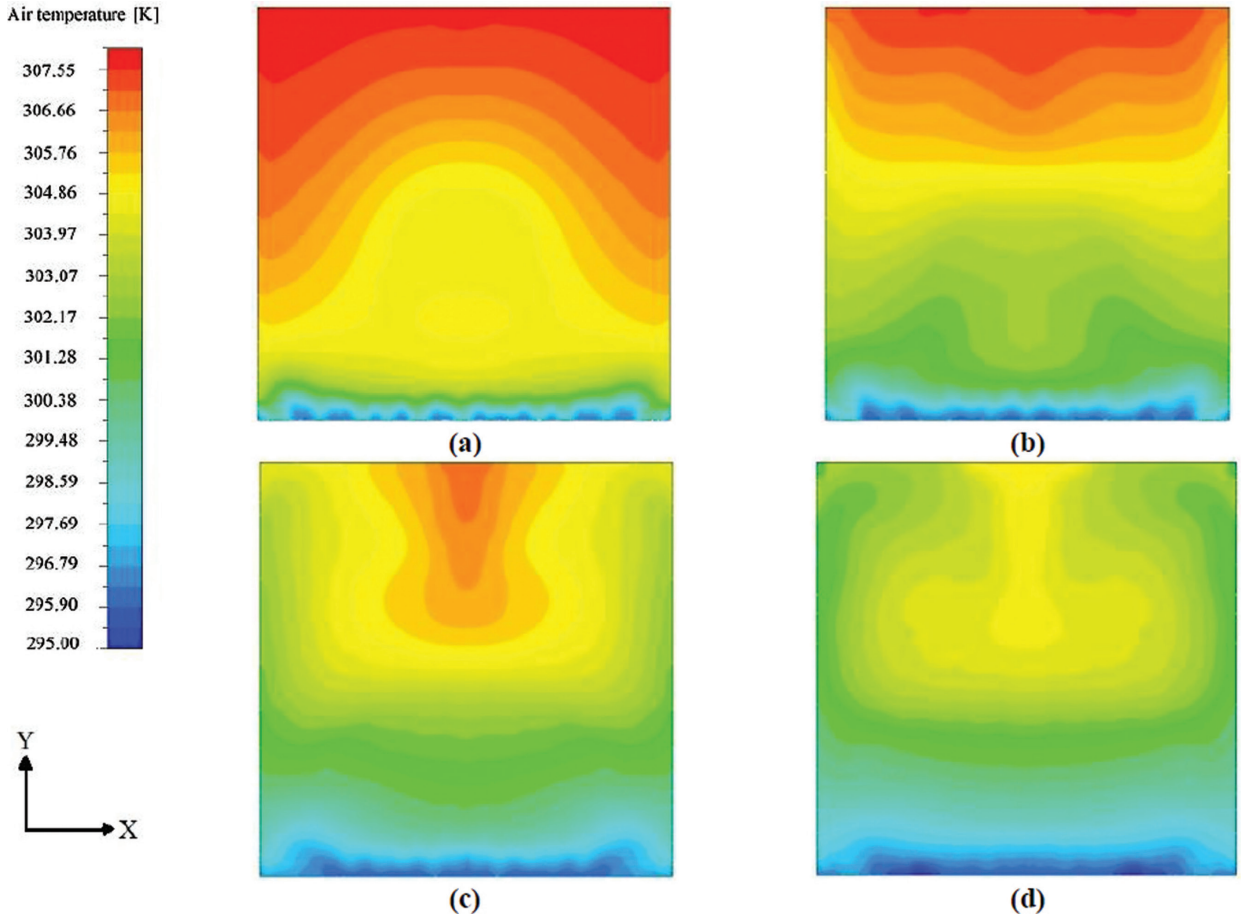

Figure 7. Air temperature profile at outlet cross section plane for one nozzle at the z = 0.2 m and $u_{a,in}$ = 1 *m/s* for various mass flow rate of water including (a) $\dot{m}_w$ = 5 l/h, (b) $\dot{m}_w$ = 10 l/h, (c) $\dot{m}_w$ = 15 l/h, and (d) $\dot{m}_w$ = 20 l/h.

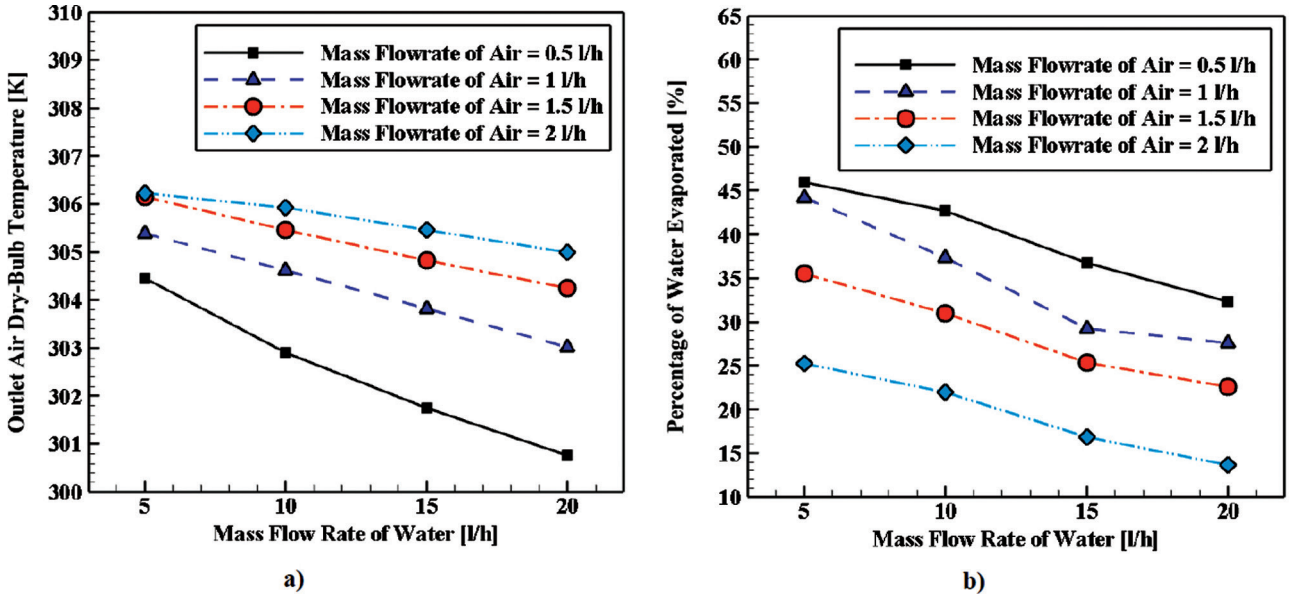

Figure 8. Predicted (a) outlet air temperature and (b) percent of water evaporated for various air and water mass flow rates.

time in the duct, they have less opportunity to evaporate in the interaction to hot air flow.

The variation of the spray cooling efficiency at different water mass flow rates and various numbers of the nozzles is depicted in Figure 6. Accordingly, it can be seen that growth in the number of the nozzles from 1 to 4 (by 300%) causes reduction in the slope of variation of spray cooling efficiency reduces, such a way that, the difference between spray cooling efficiency at 3 and 4 number of nozzles is less than 1.8%. In other words, at a constant water mass flow rate, when the number of the nozzles increases, the spray cooling efficiency declines.

For instance, at the case with N=1, by increasing the mass flow rate of water from 5 to 20 l/h (300% growth), the spray cooling efficiency rises from 17.2% to 37.2% (116.28 growth). Moreover, at high mass flow rate of water in which the differences between the models are significant, by increasing the number of nozzles from one to two (100% growth), three (200% growth), and four (300% growth), the spray cooling efficiency decline by 9.68%, 17.2%, and 18.28%, respectively. Obtained results show obviously that the difference between cases with N = 3 and N = 4 is very low. The maximum and minimum spray cooling efficiency belong to the cases with N = 1 at $\dot{m}_{Water}$ = 20 l/h and N = 4 at $\dot{m}_{Water}$ = 5 l/h, respectively.

The outlet cross section plane temperature contours, for one nozzle located at z = 0.2 m, are shown in Figure 7 for different mass flow rates of 5 l/h to 20 l/h. As the nozzle is located at x = 33.75 cm which is the center of cross section width, the geometry and the other condition is symmetric and this is obvious in contours. The center and bottom of the cross section is more influenced by spray cooling this is because of gravity and the nozzle location.

EFFECT OF THE INLET AIR MASS FLOW RATE

Inlet air velocity obviously plays an important role on evaporative cooling process. In the present section, the impact of inlet air mass flowrate on the evaporative cooling process is evaluated numerically. Four various inlet air mass flowrate are considered here including 0.5, 1, 1.5, and 2 l/h. The influence of inlet air velocity on the outlet air dry-bulb temperature and percent of water evaporated for various water mass flowrates are depicted in Figures 8(a) and 8(b), respectively.

Figure 8(a) illustrates that as the water mass flowrate rises, outlet air dry-bulb temperature decline which this trend is the same for all evaluated cases with various air mass flowrate. Moreover, it can be concluded that the differences between the cases (with various air mass flowrate) expand at higher water mass flowrate. For instance, at lower water mass flowrate ($\dot{m}_{Water}$ = 5 l/h), by increasing the air mass flowrate from 0.5 to 2 l/h (growth by about 300%), the outlet air dry-bulb temperature rises by 0.6%. Also, at higher water mass flowrate ($\dot{m}_{Water}$ = 20 l/h), growth in the air mass flowrate by about 300% causes an augmentation in the outlet air dry-bulb temperature by about 1.4%.

According to Figure 8(b), it can be realized that augmentation in the water mass flowrate makes the percentage of evaporated water to be declined which the trend is identical for all cases with various air mass flowrate. Furthermore,

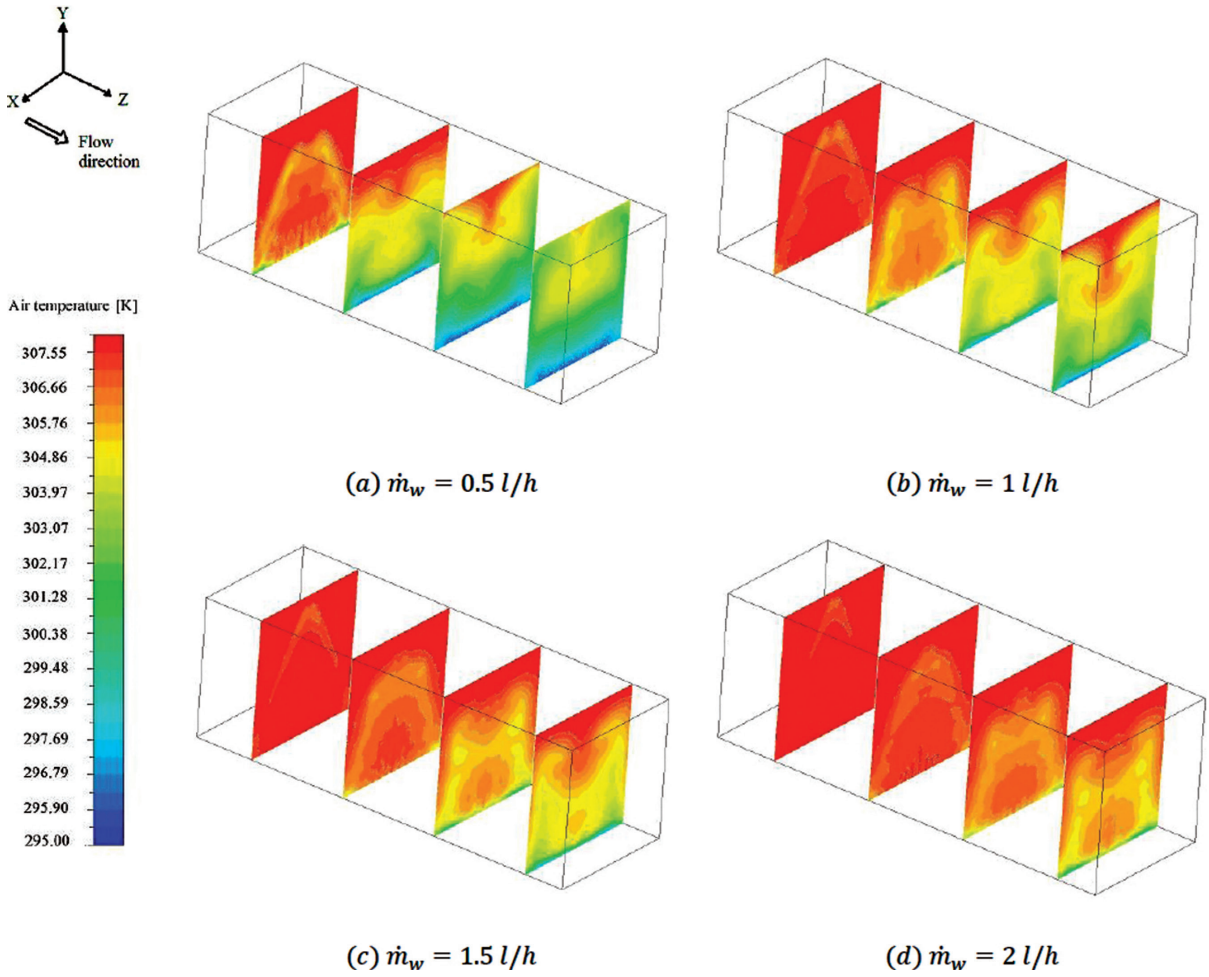

Figure 9. Contours of air temperature in four slices (X direction) inside the duct for different inlet air flow from (a) 0.5 l/h to (d) 2 l/h at $N = 4$, $\dot{m}_w = \frac{5L}{h}$ for each nozzle.

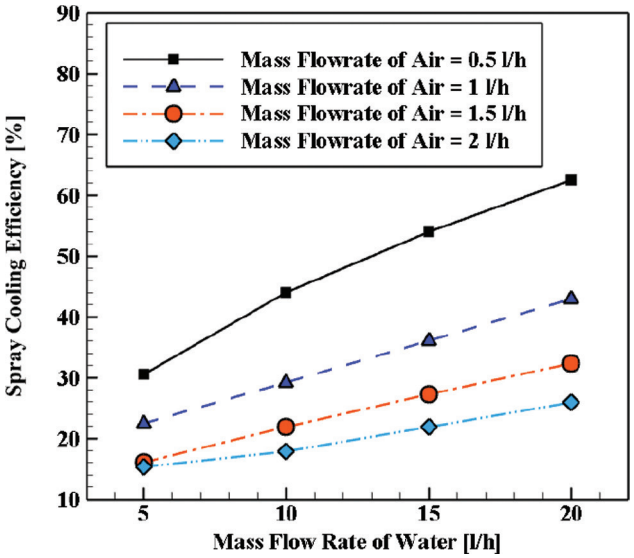

Figure 10. Variation of spray cooling efficiency for various water mass flow rate and inlet air velocity.

in all evaluated water mass flowrate, as the air mass flowrate rises, the percentage of evaporated water decreases. For example, at lower water mass flowrate ($\dot{m}_{Water}$ = 5 l/h), by increasing the air mass flowrate from 0.5 to 2 l/h (growth by about 300%), the percentage of evaporated water declines by about 84%. Moreover, at higher water mass flowrate ($\dot{m}_{Water}$ = 20 l/h), growth in the air mass flowrate by about 300% causes an increase in percentage of evaporated water by about 56.25%.

Contours of air dry bulb temperature in four slices (X direction) of the channel for various inlet air mass flow from 0.5 l/h to 2 l/h is displayed in Figure 9. The slices have been selected at 0.3, 0.8, 1.3, and 1.8 m distance from the inlet of channel. It can be obviously realized that the outlet air temperature is declined by decrease of air velocity, because when the inlet air velocity for example is 0.5 m/s, the residence time of air in the channel is at least 4 times more than the case with inlet air velocity of 2 m/s, therefore the droplets and airflow have more time to influence on each other so the momentum and energy exchange between

water particles and air is more resulting droplet evaporation and sensible heat transfer will be enhanced.

The contours also represent that the coverage area which influenced by the spray cooling is concentrated at the bottom. This observation has two reasons: first the spray injection direction is from top to bottom so the water droplet concentration is more at the lower parts of the duct and the second is the gravitational force which is exerted to the bottom so air and droplets are attracted to bottom. The interaction between airflow and the droplets causes penetration of spray cooling to the top of the cross sections and the coverage area gradually promotes to the top as it is clear in the profiles.

The variation of the spray cooling efficiency at different water mass flow rates and various air mass flow rates is illustrated in Figure 10. Consequently, it can be realized that growth in the air mass flow rate from 0.5 l/h to 2 l/h (by 300%) makes decrease in the spray cooling efficiency in all investigated water mass flow rates. Also, it can be concluded that as the water mass flowrate rises, the spray cooling efficiency rises in all evaluated air mass flow rates.

For example, at the case with air mass flow rate equal to 0.5 l/h ($\dot{m}_{Air}$ = 0.5 l/h), by increasing the mass flow rate of water from 5 to 20 l/h (300% growth), the spray cooling efficiency increases from about 30% to 62% (106.67% growth). Furthermore, at high mass flow rate of water in which the differences between the models are major, by increasing the air mass flowrate from 0.5 l/h to 1 l/h (100% growth), 1.5 l/h (200% growth), and 2 l/h (300% growth), the spray cooling efficiency decline by about 32.26%, 48.39%, and 58.06%, respectively. The maximum and minimum spray cooling efficiency belong to the cases with $\dot{m}_{Air}$ = 0.5 l/h at $\dot{m}_{Water}$ = 20 l/h and $\dot{m}_{Air}$ = 2 l/h at $\dot{m}_{Water}$ = 5 l/h, respectively.

CONCLUSION

In the present work, an Eulerian–Lagrangian 3D CFD model was developed to investigate the influence of important parameters on spray cooling performance in a rectangular duct. The evaluated parameters include the number of water nozzles, the inlet air mass flowrate, and the sprayed water mass flowrate. The major results of this investigation are as follows:

- Growth in the number of the nozzles causes reduction in the spray cooling efficiency.
- The maximum and minimum spray cooling efficiency belong to the cases with N = 1 at $\dot{m}_{Water}$ = 20 l/h and N = 4 at $\dot{m}_{Water}$ = 5 l/h, respectively.
- Moreover, increasing the air mass flow rate from 0.5 l/h to 2 l/h (by 300%) makes decrease in the spray cooling efficiency in all investigated water mass flowrates.
- The highest and lowest spray cooling efficiency belong to the cases with $\dot{m}_{Air}$ = 0.5 l/h at $\dot{m}_{Water}$ = 20 l/h and $\dot{m}_{Air}$ = 2 l/h at $\dot{m}_{Water}$ = 5 l/h, respectively.

NOMENCLATURE

C_D	Drag coefficient
D_d	Droplet diameter, [μm]
g	Gravitational acceleration, [m/s]
E	Total energy, [J]
F_D	Drag force, [N]
h_c	Heat transfer coefficient, [$W/(m^2.K)$]
h_d	Mass transfer coefficient, [m/s]
h_{fg}	Latent heat of water vaporization, [J/kg]
K	Thermal conductivity, [$W/(m.K)$]
$\dot{m}_W$	Water mass flow rate, [kg/s]
m_d	Droplet mass, [kg]
Nu	Nusselt number, [nd]
P	Pressure, [Pa]
Re_d	Droplet Reynolds number, [nd]
RH	Relative humidity, [%]
S_e	Source term of energy, [W/m^3]
S_m	Source term of mass, [$kg/(m^3.s)$]
S_{mo}	Source term of momentum, [$kg/(m^2.s^2)$]
T	Temperature, [K]
u_a	Air velocity, [m/s]
v_d	droplet velocity, [m/s]
V_{cell}	Computational cell volume, [m^3]

Greek symbols

α	Nozzle cone angle, [°]
ρ	Density, [kg/m^3]
δ_{ij}	Mean strain tensor, [$1/s$]
μ	Dynamic viscosity of air, [$kg/(m.s)$]
Φ	Viscous dissipation, [W/m^3]
v	Velocity, [m/sec]
η_{sc}	Spray cooling efficiency

Subscripts

a	air
d	Droplet
w	water
v	vapor
i, j, k	Cartesian coordinate direction
wb	Wet-bulb

AUTHORSHIP CONTRIBUTIONS

Authors equally contributed to this work.

DATA AVAILABILITY STATEMENT

The authors confirm that the data that supports the findings of this study are available within the article. Raw

data that support the finding of this study are available from the corresponding author, upon reasonable request.

CONFLICT OF INTEREST

The author declared no potential conflicts of interest with respect to the research, authorship, and/or publication of this article.

ETHICS

There are no ethical issues with the publication of this manuscript.

REFERENCES

[1] Wataru N, Heikichi K, Shigeki H. Heat transfer from tube banks to air/water mist flow. Int J Heat Mass Transf 1988;31:449-460. [CrossRef]

[2] Hou Y, Tao Y, Huai X, Zou Y, Sun D. Numerical simulation of multi-nozzle spray cooling heat transfer. Int J Therm Sci 2018;125:81-88. [CrossRef]

[3] Islam MR, Jahangeer KA, Chua KJ. Experimental and numerical study of an evaporatively-cooled condenser of air-conditioning systems. Energy 2015;87:390-399. [CrossRef]

[4] Deshmukh A. Design, development and fabrication of a mist spray direct evaporative cooling system and its performance evaluation. J Therm Eng 2019;5:42-50. [CrossRef]

[5] Tissot J, Boulet P, Trinquet F, Fournasion L, Lejeune M, Liaudet F. Improved energy performance of a refrigerating machine using water spray upstream of the condenser. Int J Refrig 2014;38:93-105. [CrossRef]

[6] Ramkumar R. Experimental investigation of indirect evaporative cooler using clay pipe. J Therm Eng 2017;3:1163-1180. [CrossRef]

[7] Keklikcioglu O, Dagdevir T, Ozceyhan V. A CFD based thermo-hydraulic performance analysis in a tube fitted with stepped conical nozzle turbulators. J Therm Eng 2016;2:913-920. [CrossRef]

[8] Chen L, Huang X, Yang L, Du X, Yang Y. Evaluation of natural draft dry cooling system incorporating water spray air precooling. Appl Therm Eng 2019;151:294-307. [CrossRef]

[9] Raoult F, Lacour S, Carrismo B, Trinquet F, Delahaye A, Fournasion L. CFD water spray model development and physical parameter study on the evaporative cooling. Appl Therm Eng 2019;149:960-974. [CrossRef]

[10] Grich N, Foudhil W, Harmand S, Jabrallah SB. Numerical simulation of water spray transport along a plate of a heat exchanger. J Therm Anal Calorim 2021;143:3887-3895. [CrossRef]

[11] Zuobing C, Qiang X, Gong C, Yongjie Y, Zheyu Z. Numerical simulation of single-nozzle large scale spray cooling on drum wall. Thermal Science 2018;22:359-370. [CrossRef]

[12] Ma, H, Si F, Zhu K, Wang J. Quantitative research of spray cooling effects on thermo-flow performance of the large-scale dry cooling tower with an integrated numerical model. Int J Heat Mass Transf 2019;141:799-817. [CrossRef]

[13] Ma H, Silaen AA, Zhou CQ. Simulation of spray cooling on hot steel slabs in continuous casting. J Therm Sci Eng Appl 2021;13:011004. [CrossRef]

[14] Wei J, Liu J, Xu X, Ruan J, Li G. Experimental and computational investigation of the thermal performance of a vertical tube evaporative condenser. Appl Therm Eng 2019;160:114100. [CrossRef]

[15] Ahmadi S, Shahrestani MI, Sayadian S, Maerefat M, Poshtiri AH. Performance analysis of an integrated cooling system consisted of earth-to-air heat exchanger (EAHE) and water spray channel. J Ther Anal Calorim 2020;143:1-11. [CrossRef]

[16] Alkhedhair A, Jahn I, Gurgenci H, Guan Z, He S. Parametric study on spray cooling system for optimising nozzle design with pre-cooling application in natural draft dry cooling towers. Int J Therm Sci 2016;104:448-460. [CrossRef]

[17] Montazeri H, Blocken B, Hensen JLM. CFD analysis of the impact of physical parameters on evaporative cooling by a mist spray system. Appl Therm Eng 2015;75:608-622. [CrossRef]

[18] Xia L, Gurgenci H, Liu D, Guan Z, Zhou L, et al. CFD analysis of pre-cooling water spray system in natural draft dry cooling towers. Appl Therm Eng 2016;105:1051-1060. [CrossRef]

[19] Omidvar A, Mahdavi A, Mehryar R. A simulated study on the effect of water temperature on cooling efficiency of water mist fire extinguishers. J Therm Eng 2020;6:460-473. [CrossRef]

[20] Heidarnejad G, Moghaddam MRA, Pasdarshahri H. Enhancing COP of an air-cooled chiller with integrating a water mist system to its condenser: Investigating the effect of spray nozzle orientation. Int J Therm Sci 2019;137:508-525. [CrossRef]

[21] Xiao L, Ge Z, Yang L, Du X. Numerical study on performance improvement of air-cooled condenser by water spray cooling. Int J Heat Mass Transf 2018;125:1028-1042. [CrossRef]

[22] Han Z, Ji Q, Wei H, Xue D, Sun X, Zhang X, Li X. Simulation study on performance of data center air-conditioning system with novel evaporative condenser. Energy 2020;210:118521. [CrossRef]

[23] Alkhedhair A, Gurgenci H, Zhiqiang G, He S. Numerical simulation of water spray for pre-cooling of inlet air in natural draft dry cooling towers. Appl Therm Eng 2013;61:416-424. [CrossRef]

[24] Hou Y, Tao Y, Huai X, Zou Y, Sun D. Numerical simulation of multi-nozzle spray cooling heat transfer. Int J Therm Sci 2018;125:81-88. [CrossRef]
[25] Li Ji, Kawano H. Simulating water-drop movement from noncircular sprinkler nozzles. J Irrig Drain Eng 1995;121:152-158. [CrossRef]
[26] Khan AR, Richardson JF. The resistance to motion of a solid sphere in a fluid. Chem Eng Commun 1987;62:135-150. [CrossRef]
[27] Haider A, Levenspiel O. Drag coefficient and terminal velocity of spherical and nonspherical particles. Powder Technol 1989;58:63-70. [CrossRef]
[28] Kelbaliev G, Ceylan K. Development of new empirical equations for estimation of drag coefficient, shape deformation, and rising velocity of gas bubbles or liquid drops. Chem Eng Commun 2007;194:1623-1637. [CrossRef]
[29] Morsi SAJ, Alexander AJ. An investigation of particle trajectories in two-phase flow systems. J Fluid Mech 1972;55:193-208. [CrossRef]
[30] Palaszewski SJ, Jiji LM, Weinbaum S. A three-dimensional air-vapor-droplet local interaction model for spray units. 1981;103:514-521. [CrossRef]
[31] Ho Y-S. Top-cited articles in chemical engineering in Science Citation Index Expanded: A bibliometric analysis. Chinese J Chem Eng 2012;20:478-488. [CrossRef]
[32] Husted, Bjarne Paulsen. Experimental Measurements of Water Mist Systems and Implications for Modelling i CFD. Department of Fire Safety Engineering, Lund University, 2007.
[33] Afsharpanah F, Sheshpoli AZ, Pakzad K, Mousavi SS. Numerical investigation of non-uniform heat transfer enhancement in parabolic trough solar collectors using dual modified twisted-tape inserts. J Therm Eng 2021;7:133-147. [CrossRef]
[34] Saedodin S, Zaboli M, Ajarostaghi SSM. Hydrothermal analysis of heat transfer and thermal performance characteristics in a parabolic trough solar collector with Turbulence-Inducing elements. Sust Energy Technol Assess 2021;46:101266. [CrossRef]
[35] Abbaspour M, Mousavi Ajarostaghi SS, Hejazi Rad SA, Nimafar M. Heat transfer improvement in a tube by inserting perforated conical ring and wire coil as turbulators. Heat Transfer 2021;50: 6164-6188. [CrossRef]
[36] Zaboli M, Saedodin S, Mousavi Ajarostaghi SS, Nourbakhsh M. Numerical evaluation of the heat transfer in a shell and corrugated coil tube heat exchanger with three various water-based nanofluids. Heat Transfer 2021;50:6043-6067. [CrossRef]
[37] Afsharpanah, F, Sheshpoli A Z, Pakzad K, Ajarostaghi SSM. Numerical investigation of non-uniform heat transfer enhancement in parabolic trough solar collectors using dual modified twisted-tape inserts. J Therm Eng 2021;7:133-147. [CrossRef]
[38] Kazemi Moghadam H, Mousavi Ajarostaghi SS, Poncet S. Numerical modeling of an innovative arc shape rib based solar air heater. Proceedings of the Institution of Mechanical Engineers, Part C: Jour nal of Mechanical Engineering Science. 2021;235:7992-8012. [CrossRef]
[39] Zaboli M, Ajarostaghi, SSM, Saedodin S, Kiani B. Hybrid nanofluid flow and heat transfer in a parabolic trough solar collector with inner helical axial fins as turbulator. Eur Phys J Plus 2021;136:841.
[40] Zaboli M, Mousavi Ajarostaghi SS, Saedodin S, Saffari Pour M. Thermal performance enhancement using absorber tube with inner helical axial fins in a parabolic trough solar collector. Appl Sci 2021;11:7423. [CrossRef]
[41] Sureshkumar R, Kale SR, Dhar PL. Heat and mass transfer processes between a water spray and ambient air–I. Experimental data. Appl Therm Eng 2008;28:349-360. [CrossRef]